

NACA RM SE54J06

~~CONFIDENTIAL~~

~~CANCELLED~~



# RESEARCH MEMORANDUM

for the

Bureau of Aeronautics, Department of the Navy

PRELIMINARY ALTITUDE PERFORMANCE DATA OF J71-A2

TURBOJET ENGINE AFTERBURNER

By James W. Useller and William E. Mallett

Lewis Flight Propulsion Laboratory  
Cleveland, Ohio

Restriction/Classification

Cancelled

This material contains information of the espionage laws, Title 18, U.S.C., in such a manner to unauthorized person

the United States within the meaning of the espionage laws, Title 18, U.S.C., in such a manner to unauthorized person

## NATIONAL ADVISORY COMMITTEE FOR AERONAUTICS

WASHINGTON

FILE COPY

To be returned to the Director, National Advisory Committee for Aeronautics, Washington, D.C.

OCT 22 1954

~~CONFIDENTIAL~~

18

**CLASSIFICATION CANCELLED**  
CONFIDENTIAL  
AUTHORITY: NASA PUBLICATIONS  
ANNOUNCEMENTS NO.  
Date \_\_\_\_\_ By \_\_\_\_\_

NATIONAL ADVISORY COMMITTEE FOR AERONAUTICS

RESEARCH MEMORANDUM

for the

Bureau of Aeronautics, Department of the Navy  
PRELIMINARY ALTITUDE PERFORMANCE DATA OF J71-A2  
TURBOJET ENGINE AFTERBURNER

By James W. Useller and William E. Mallett

SUMMARY

The performance and operational characteristics of the J71-A2 turbojet-engine afterburner were investigated for a range of altitudes from 23,000 to 60,000 feet at a flight Mach number of 0.9 and at flight Mach numbers of 0.6, 0.9, and 1.0 at an altitude of 45,000 feet. The combustion performance and altitude operational limits, as well as the altitude starting characteristics have been determined.

INTRODUCTION

At the request of the Bureau of Aeronautics, Department of the Navy, an investigation of the performance and operational characteristics of the J71-A2 turbojet engine afterburner was undertaken in an NACA Lewis laboratory altitude test chamber. A prior investigation of the unaugmented performance of the J71-A2 engine is reported in reference 1.

The afterburner performance was investigated for a range of altitudes from 23,000 to 60,000 feet at a flight Mach number of 0.9 and for flight Mach numbers of 0.6, 0.9, and 1.0 at an altitude of 45,000 feet and is presented herein. The combustion temperature and efficiency of the afterburner have been determined for a range of altitudes at a flight Mach number of 0.9. The operational limits of maximum altitude, lean blow-out, and maximum equivalence ratio have been determined, as well as the altitude starting characteristics of the afterburner.

APPARATUS AND PROCEDURE

Afterburner configuration. - The J71-A2 afterburner has a nominal length of 11 feet and diameter of 40 inches. A schematic diagram of

**CLASSIFICATION CANCELLED**  
CONFIDENTIAL  
AUTHORITY: NASA PUBLICATIONS

REF 1

T-20

the afterburner showing the location of the various components is presented in figure 1. A photograph of the afterburner and engine installed in the altitude test chamber is shown in figure 2. A sketch of the afterburner showing the ignitors, flame holder, and fuel spray system is shown in figure 3(a).

Two afterburner ignitors were located  $180^\circ$  apart immediately downstream of the turbine outlet. The ignitor was a tube with seven orifices equally spaced radially. A photograph of one of the ignitors is shown in figure 3(b). Ignition was accomplished by providing a momentary supply of fuel through the orifices. For comparative purposes, an NACA "hot-streak" ignitor was also used during this investigation. The NACA ignitor consisted of a single atomizing nozzle which supplied a momentary burst of fuel into a localized region of the combustor immediately upstream of the turbine.

The afterburner fuel system consisted of 22 dual spray bars (shown in fig. 3(c)) equally spaced circumferentially at a station 8.5 inches upstream of the flame holder. Each portion of the dual spray bar was separately manifolded and provided with a flow divider that controlled the fuel distribution according to the pressure necessary for good atomization. During this investigation the fuel-flow rates and supply pressures were such that only the primary segment of each spray bar was used.

The flame holder was of the 2-ring, staggered V-gutter type, and blocked 30 percent of the annular area. A sketch of the flame holder is shown in figure 3(a). The average gas velocity at the afterburner inlet was 370 feet per second.

The afterburner cooling liner was corrugated to increase its strength and was perforated from the flame holder to a distance 32 inches downstream of the flame holder. Cooling air ducted from the turbine discharge flowed through the perforated section of the afterburner wall into the combustion chamber. The afterburner exhaust nozzle had a continuously variable area that ranged from approximately 2.5 to 4.5 square feet. An afterburner control system consisting of an amplifier and a servo-valve actuator continually adjusted the exhaust-nozzle area to maintain a maximum turbine discharge gas temperature of  $1670^\circ$  R as indicated by the manufacturer's thermocouples.

Engine and installation. - The afterburner investigated is an integral part of the J71-A2 turbojet engine. The investigation was conducted in an NACA altitude test chamber in which pressures and temperatures simulating altitude flight conditions were supplied to the engine inlet. Altitude pressures were simulated at the engine exhaust.

The engine has a bifurcated inlet, a 16-stage, axial-flow compressor, a canular-type combustor, and a 3-stage turbine. The engine has a

nominal unaugmented thrust rating of 10,200 pounds while operating at a rotor speed of 6100 rpm and a turbine discharge gas temperature of 1670° R as indicated by the manufacturer's thermocouples.

Fuel conforming to MIL-F-5624a (grade JP-4) specification was used in both the engine and the afterburner. The lower heating value of the fuel was 18,700 Btu per pound and the hydrogen-carbon ratio was 0.169.

Instrumentation. - The afterburner inlet conditions were surveyed by 25 total-pressure and 25 total-temperature probes in addition to 12 manufacturer's thermocouples. When an average gas temperature of 1670° R was indicated by the manufacturer's thermocouples, the more complete survey with the 25 NACA thermocouples averaged only 1620° R. The cooling air-flow rate was measured in the afterburner cooling shroud by four total-pressure probes and a single stream static-pressure probe. A water-cooled rake at the exhaust-nozzle inlet containing 14 total-pressure probes placed on centers of equal area provided a survey of the afterburner exhaust conditions. The ejector passage was instrumented with nine total-pressure, three static-pressure, and three thermocouple probes.

Standard engine instrumentation was provided to measure the air flow, engine fuel flow, and thrust. A detailed description of the engine instrumentation is contained in reference 1.

Procedure. - The afterburner performance was investigated at the following simulated flight conditions with the engine operating at rated rotor speed and turbine discharge gas temperature.

<u>Altitude, ft</u>	<u>Flight Mach number</u>
23,000	0.9
35,000	0.9
45,000	0.6, 0.9, 1.0
55,000	0.9
60,000	0.9

Data were obtained at each flight condition for a range of equivalence ratios (percent of stoichiometric fuel-air ratio) from approximately 0.2 to 1.0. The range of afterburner fuel-air operation as limited by the control system was determined. Also, the maximum and minimum range of operation of the afterburner with the control system removed was investigated.

The lean limit was established by cessation of the combustion, while the rich limit was imposed by the maximum area of the exhaust nozzle. Data were obtained at these flight conditions both with and without the exhaust-nozzle ejector in position. Afterburner ignition was attempted at each flight condition with the manufacturer's ignitor and the NACA "hot-streak" ignitor.

A list of the symbols used in this report is contained in appendix A and an explanation of the method of calculations is presented in appendix B.

#### DATA PRESENTATION

The experimental data are grouped according to the index presented in table I. The over-all engine-afterburner performance in terms of augmented net thrust ratio and specific fuel consumption is presented in figure 4. The afterburner performance is presented in figures 5 and 6. To obtain sufficient data to compute the combustion temperature and efficiency of figure 6, it was necessary to remove the ejector configuration. It was therefore possible to evaluate the jet thrust loss imposed by installation of the ejector; this ejector-induced thrust loss is shown in figure 7.

Afterburner operational characteristics are shown in figures 8 to 10. The maximum operable altitude and range of operable equivalence ratio are shown in figure 8. The limits of operation imposed by the afterburner control system have been included on the figure to permit comparison with the region of operation possible with manual throttle control.

The afterburner altitude starting limits using the manufacturer's ignitor and the NACA "hot-streak" ignitor are compared in figure 9. The afterburner operational limits have been superimposed on this figure.

Representative longitudinal temperature distributions along the afterburner shell are shown in figure 10. The decrease in wall temperature approximately 90 inches downstream of the burner inlet is due to the cooling provided by the exhaust-nozzle ejector. The ejector cooling flow was approximately 1.5 percent of engine flow, and the afterburner internal shell cooling flow rate was between 3 and 6 percent of the engine air flow.

A tabulation of the performance data obtained in this investigation is presented in table II.

Lewis Flight Propulsion Laboratory  
National Advisory Committee for Aeronautics  
Cleveland, Ohio, October 7, 1954

## APPENDIX A

## SYMBOLS

The following symbols are used in this report:

$C_j$	nozzle flow coefficient
$F_e$	unaugmented engine net thrust, lb
$F_j$	augmented jet thrust, lb
$F_n$	augmented net thrust, lb
$f/a$	fuel-air ratio
$g$	acceleration due to gravity, 32.17 ft/sec <sup>2</sup>
$M$	Mach number
$P$	total pressure, lb/sq ft abs
$p$	static pressure, lb/sq ft abs
$R$	gas constant, $\frac{1546 \text{ ft-lb}}{(\text{molecular wt})(\text{lb})(^{\circ}\text{R})}$
$sfc$	specific fuel consumption, lb/hr/lb
$T$	total temperature, $^{\circ}\text{R}$
$V$	velocity, ft/sec
$W_a$	air flow, lb/sec
$W_f$	fuel flow, lb/hr
$W_g$	weight flow, lb/sec
$\gamma$	ratio of specific heats
$\eta$	efficiency
$\phi$	equivalence ratio

## Subscripts:

ab afterburner  
e engine  
0 free stream  
2 compressor inlet  
3 compressor outlet  
5 turbine outlet  
9 exhaust-nozzle inlet

2557

## APPENDIX B

## CALCULATIONS

Equivalence ratio. - The afterburner equivalence ratio is defined as the percent of stoichiometric fuel-air ratio in the afterburner where the afterburner fuel-air ratio is defined as follows:

$$\left(\frac{f}{a}\right)_{ab} = \frac{\frac{W_{f,e} + W_{f,ab}}{W_{a,5}} - \left(\eta_e \frac{W_{f,e}}{W_{a,5}}\right)}{1 - \left[\frac{\eta_e \left(\frac{W_{f,e}}{W_{a,5}}\right)}{0.0674}\right]} \quad (1)$$

The equivalence ratio is then

$$\phi = \frac{(f/a)_{ab}}{0.0674} \quad (2)$$

where 0.0674 is the stoichiometric fuel-air ratio for the fuel used.

Augmented thrust ratio. - The augmented thrust ratio is based on the normal thrust of the standard engine configuration, afterburner not operating, as calculated at the same turbine-outlet conditions as the augmented thrust and introducing the 5.5-percent loss in total pressure caused by the drag in the afterburner. For the case of augmented net thrust the function is as follows:

$$F_n/F_e = \frac{\text{Net thrust with afterburning}}{\text{Normal net thrust}} \quad (3)$$

Over-all specific fuel consumption. - The over-all specific fuel consumption is based on the augmented net thrust and the sum of the engine and afterburner fuels.

Combustion efficiency. - The combustion efficiency of the afterburner was determined as a ratio of the actual to ideal temperature rise across the afterburner. The actual combustion temperature  $T_g$  was calculated



from the gas flow, the measured thrust, and a pressure survey at station 9, using the jet thrust equation as follows:

$$T_9 = \left( \frac{F_j}{W_{g,9}} \right)^2 \left( \frac{g}{C_j \sqrt{gR}} \right)^2 \left( \frac{V}{\sqrt{gRT}} \right)^{\frac{1}{2}} \quad (4)$$

Values of the effective velocity parameter  $\left( \frac{V}{\sqrt{gRT}} \right)$  were obtained from reference 2 using the appropriate values for  $\gamma_9$ . The combustion efficiency defining equation is as follows:

$$\eta_{ab} = \frac{\Delta T_{5-9}(\text{actual})}{\Delta T_{5-9}(\text{ideal})} \quad (5)$$

where the ideal temperature rise was determined by the method of reference 3.

#### REFERENCES

1. Useller, James W., and Mallett, William E.: Preliminary Altitude Performance Data for the J71-A2 (X-26) Turbojet Engine. NACA RM SE54H06, 1954.
2. Turner, L. Richard, Addie, Albert N., and Zimmerman, Richard H.: Charts for the Analysis of One-Dimensional Steady Compressible Flow. NACA TN 1419, 1948.
3. Mulready, Richard C.: The Ideal Temperature Rise Due to the Constant Pressure Combustion of Hydrocarbon Fuels. M.I.T. Meteor Rep. UAC-9, Res. Dept., United Aircraft Corp., July 1947. (BuOrd Contract NORD 9845.)

TABLE I. - FIGURE INDEX

Figure	Dependent variable	Independent variable
1	Schematic diagram of afterburner	
2	Photograph of afterburner installation	
3(a)	Afterburner component parts; flame holder and spray bars in position	
3(b)	Manufacturer's afterburner ignitor	
3(c)	Afterburner fuel spray bar	
Over-all Engine Performance		
4(a)	Augmented net thrust ratio variation with altitude	Afterburner equivalence ratio
4(b)	Over-all net thrust specific fuel consumption variation with altitude	Afterburner equivalence ratio
4(c)	Augmented net thrust ratio variation with flight Mach number	Afterburner equivalence ratio
4(d)	Over-all net thrust specific fuel consumption variation with flight Mach number	Afterburner equivalence ratio
Afterburner Performance		
5	Afterburner total pressure loss	Afterburner equivalence ratio
6(a)	Combustion temperature	Afterburner equivalence ratio
6(b)	Combustion efficiency	Afterburner equivalence ratio
Effect of Ejector on Performance		
7	Ejector jet thrust loss	Afterburner equivalence ratio
Operational Characteristics		
8	Afterburner operational limits	Afterburner equivalence ratio
9	Afterburner ignition limits	Afterburner equivalence ratio
10	Local afterburner shell temperature	Distance downstream from turbine outlet

53-4



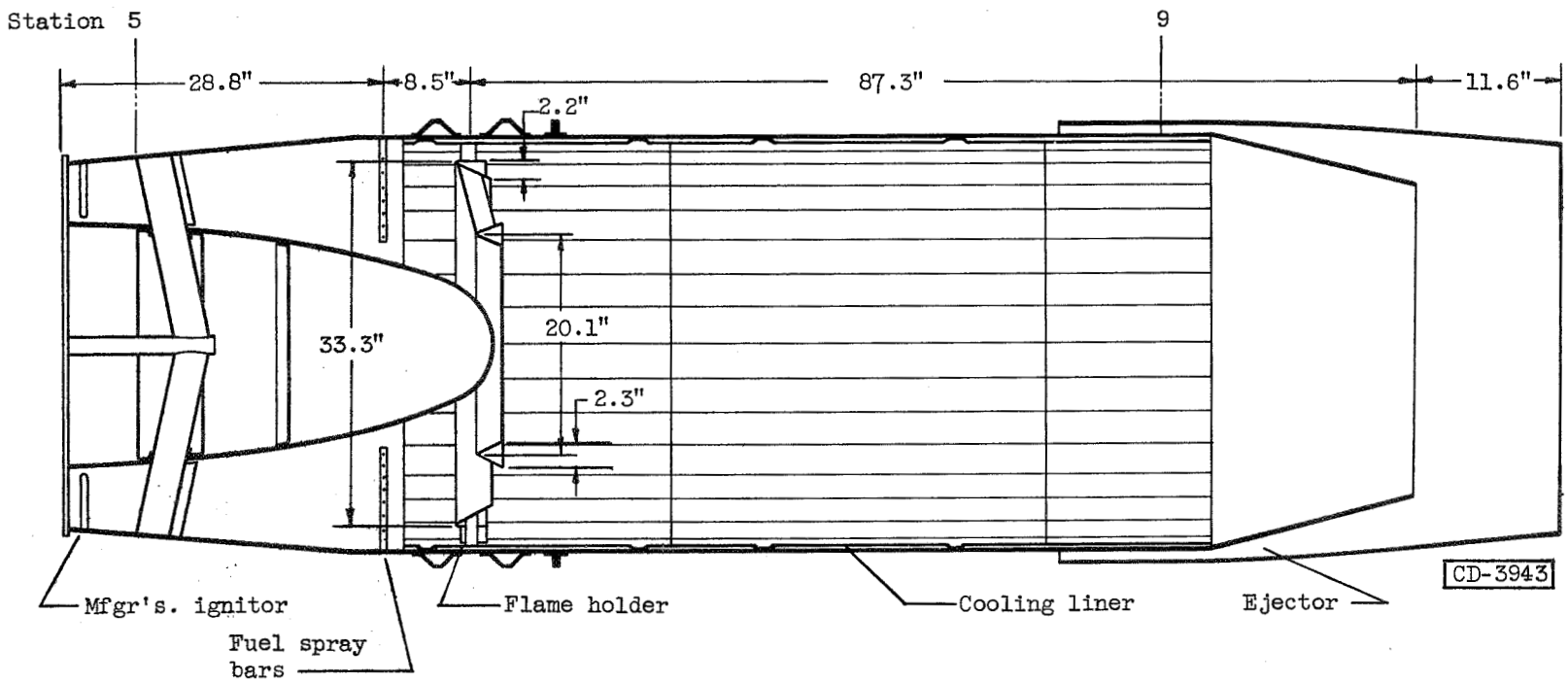


Figure 1. - Schematic diagram of J71-A2 turbojet engine afterburner showing location of various components.

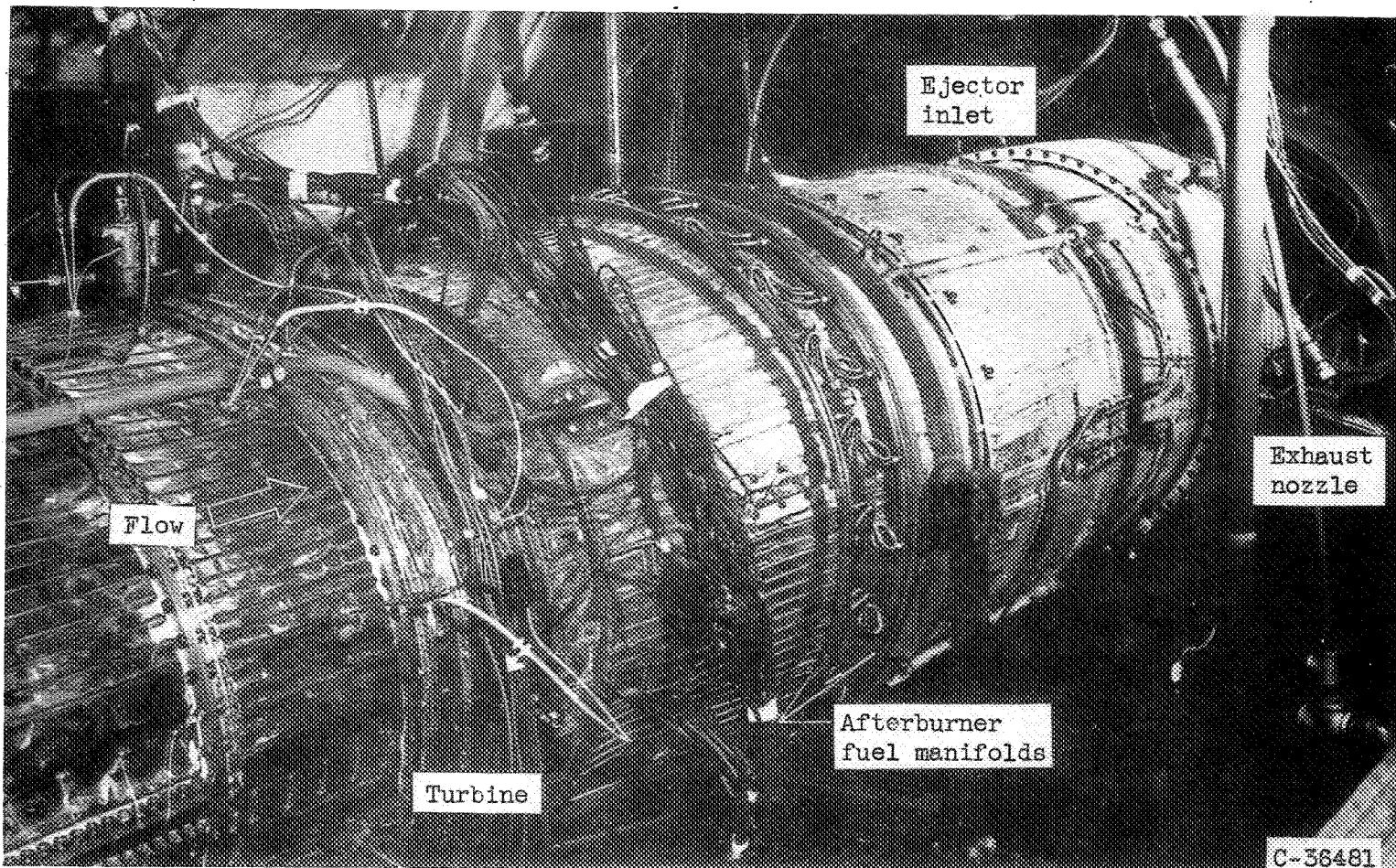
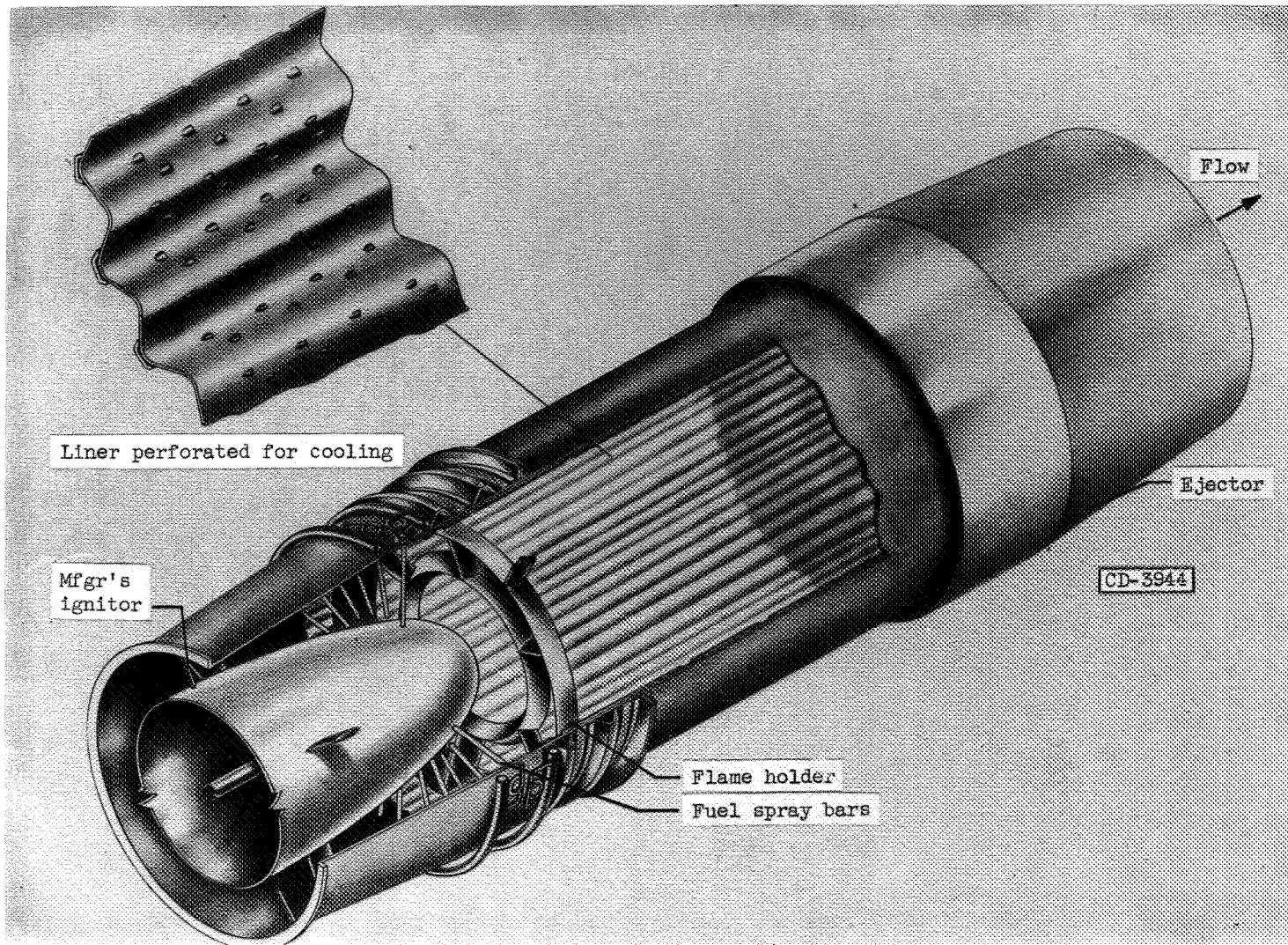
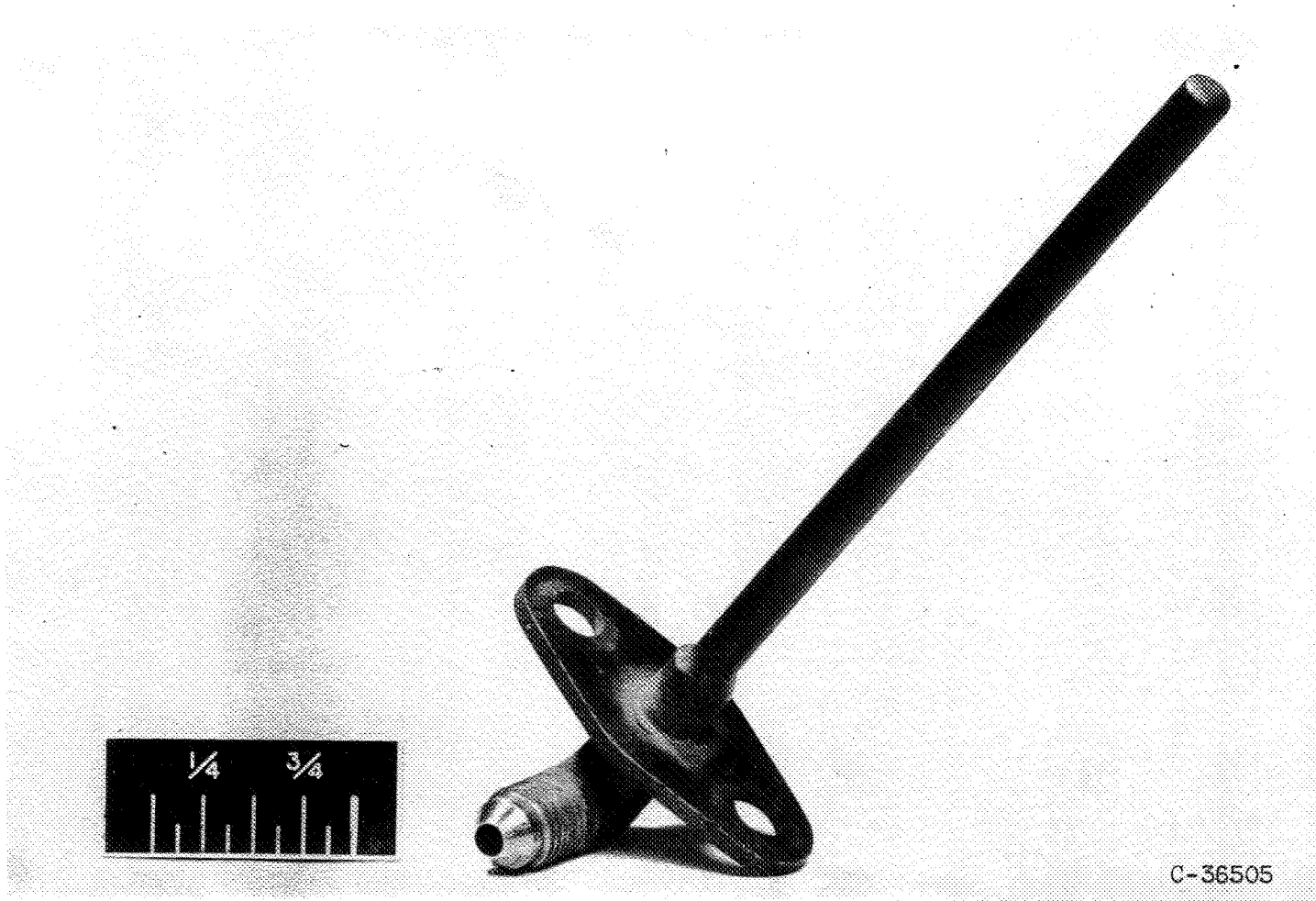


Figure 2. - J71-A2 turbojet engine afterburner installed in altitude test chamber.



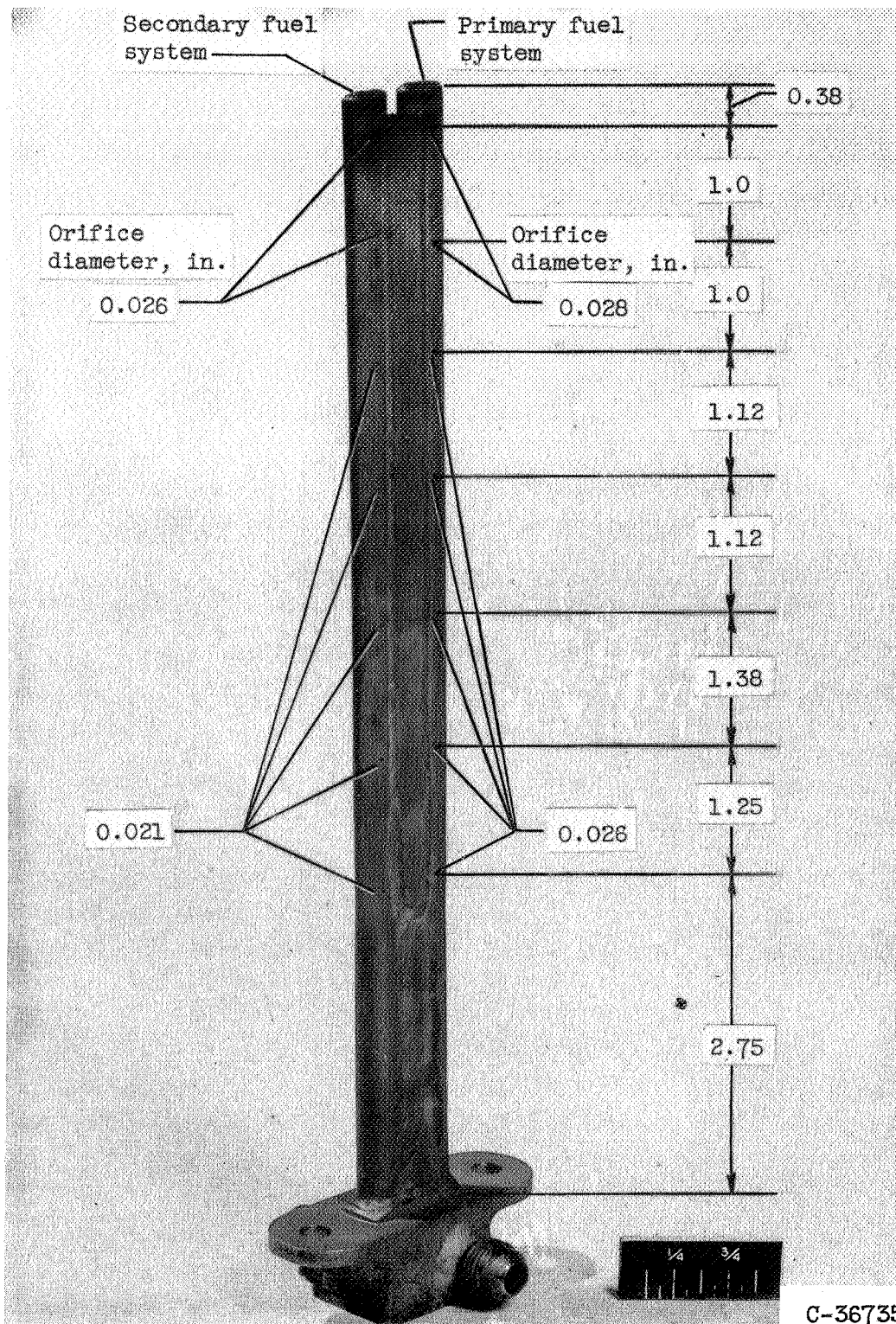
(a) Sketch showing afterburner flame holder and spray bars in position.

Figure 3. - J71-A2 turbojet engine afterburner component parts.



(b) Manufacturer's afterburner ignitor.

Figure 3. - Continued. J71-A2 turbojet engine afterburner component parts.



(c) Afterburner fuel spray bar.

Figure 3. - Concluded. J71-A2 turbojet engine afterburner component parts.



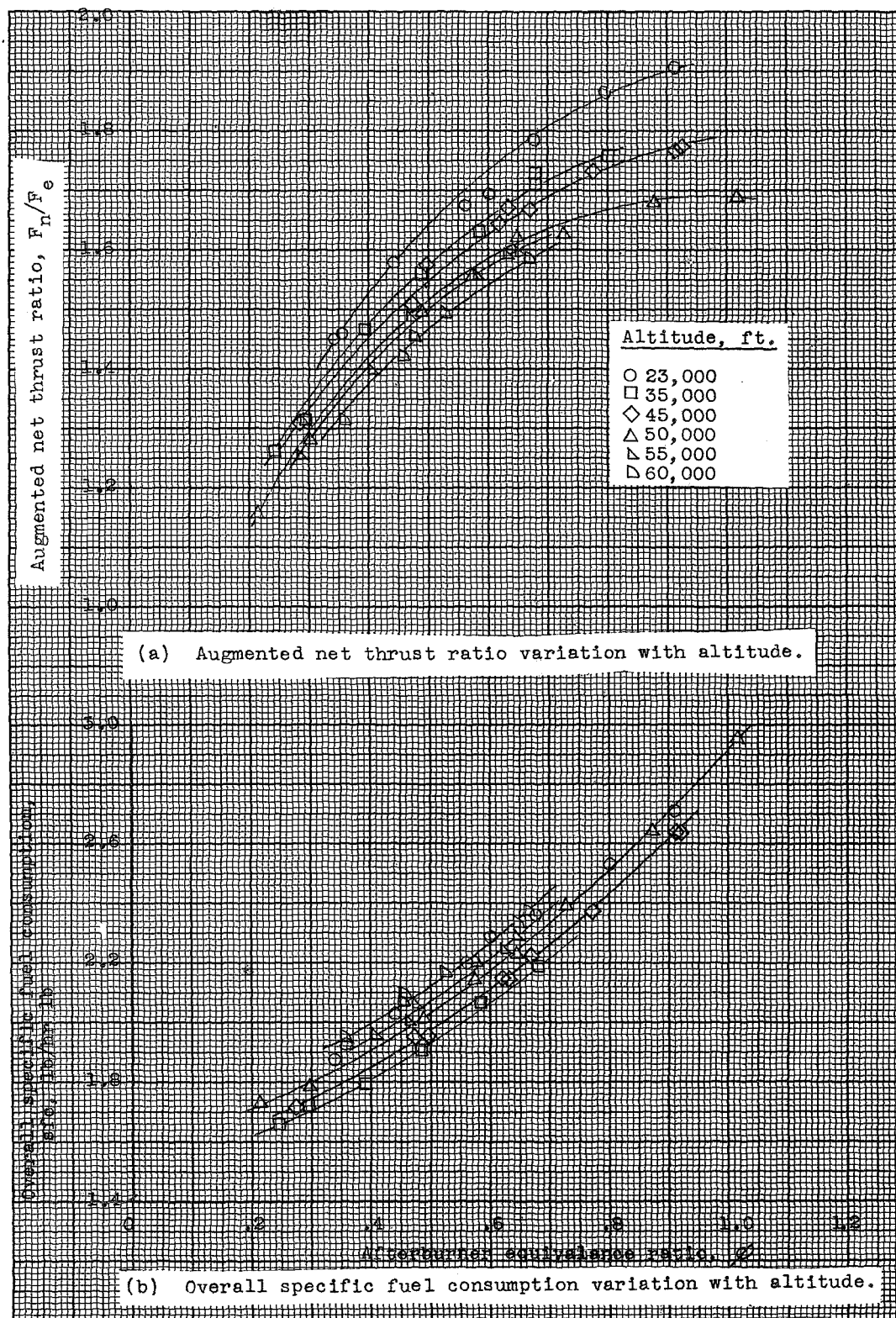
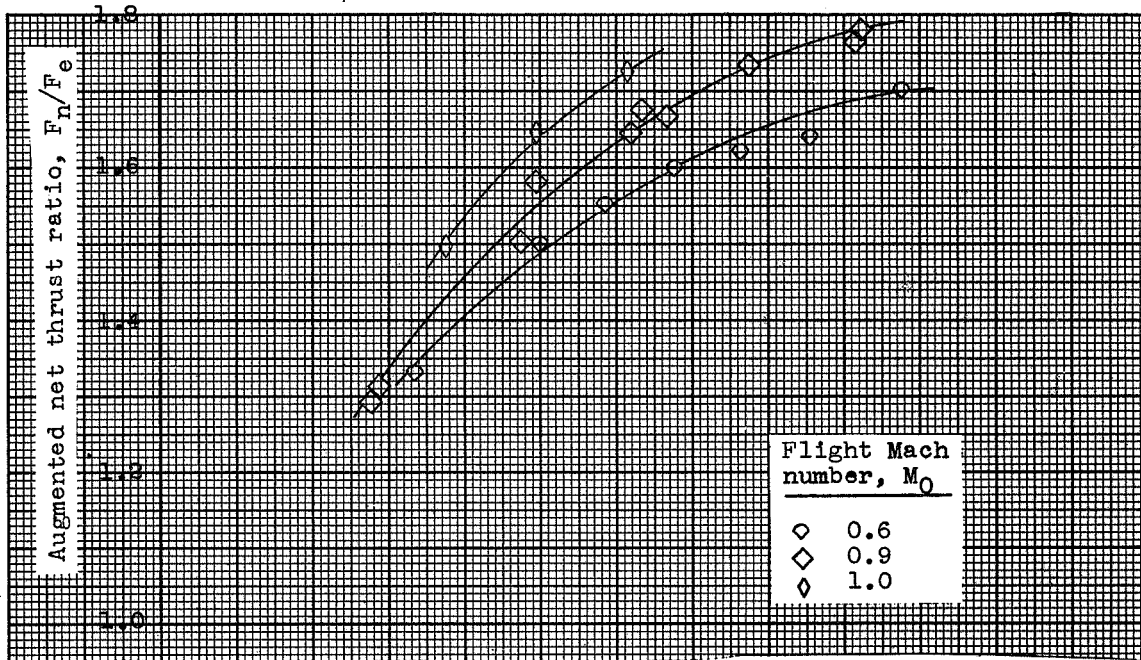
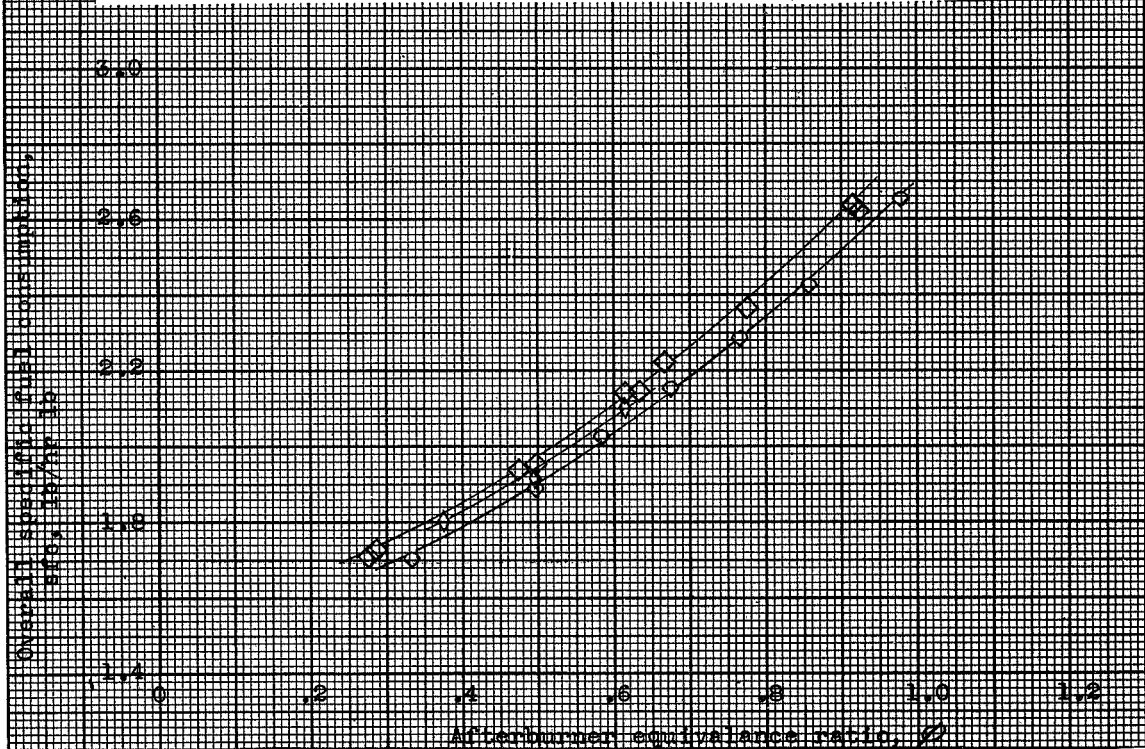


Figure 4. J71-A2 turbojet engine afterburner performance variation with altitude and flight Mach number.



(c) Augmented net thrust ratio variation with flight Mach number.



(d) Overall specific fuel consumption variation with flight Mach number.

Figure 4. J71-A2 turbojet engine afterburner performance variation with altitude and flight Mach number.

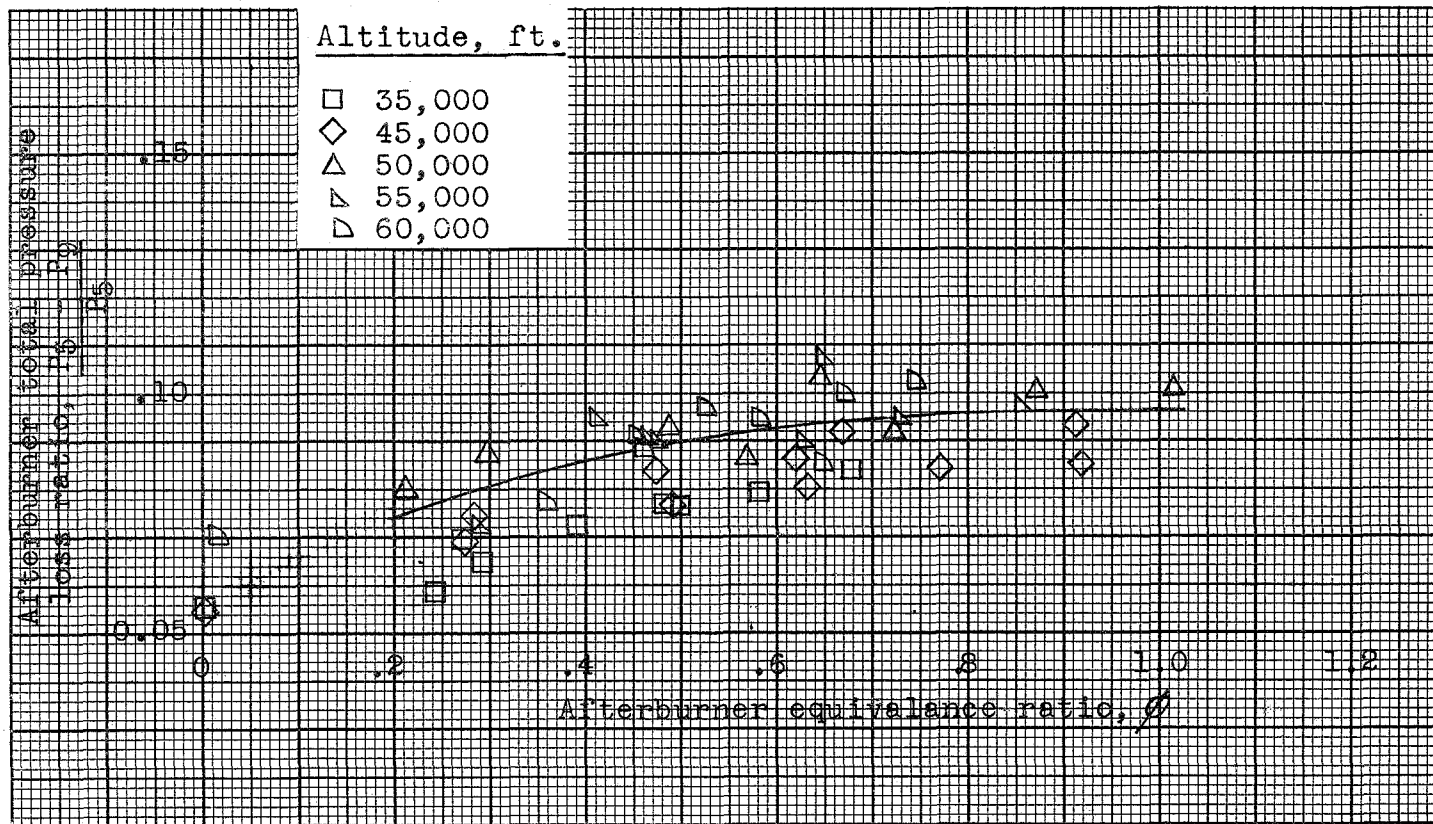


Figure 5. J71-A2 turbojet engine afterburner total pressure loss variation with afterburner equivalence ratio.

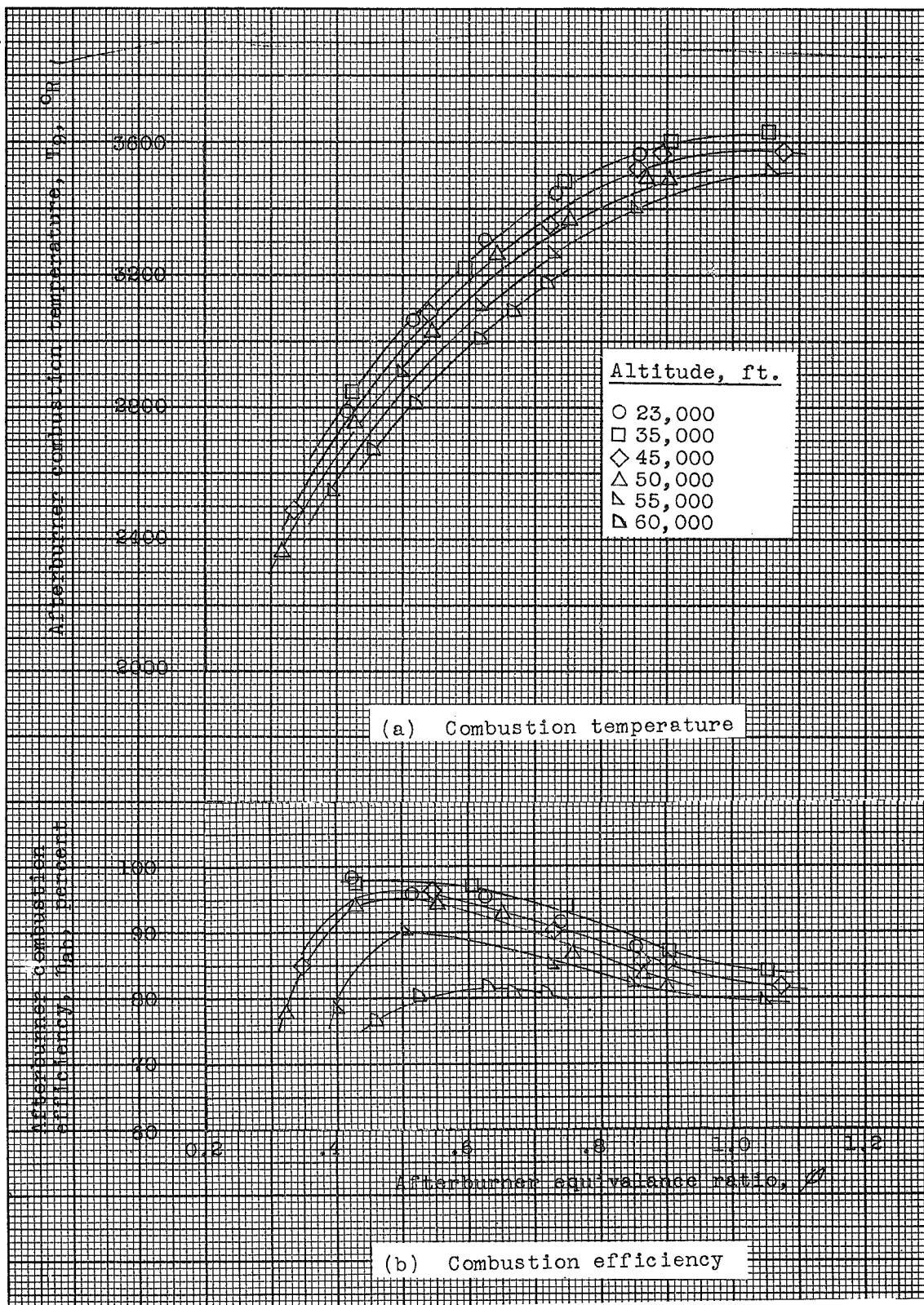


Figure 6. J71-A2 turbojet engine afterburner combustion performance variation with altitude.

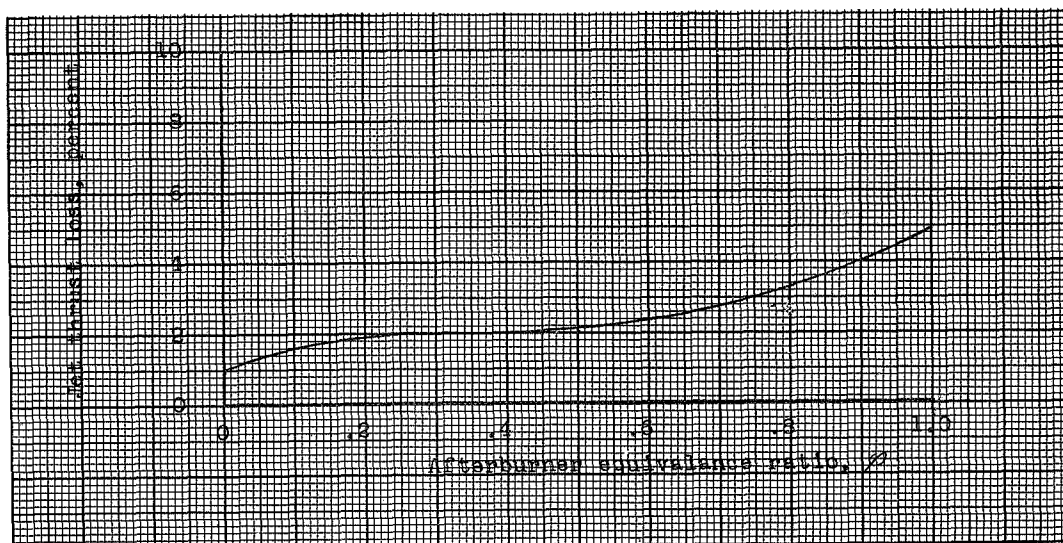


Figure 7. Jet thrust loss due to ejector configuration on J71-A2 turbojet engine afterburner.  $P_9/p_0 = 3.57$

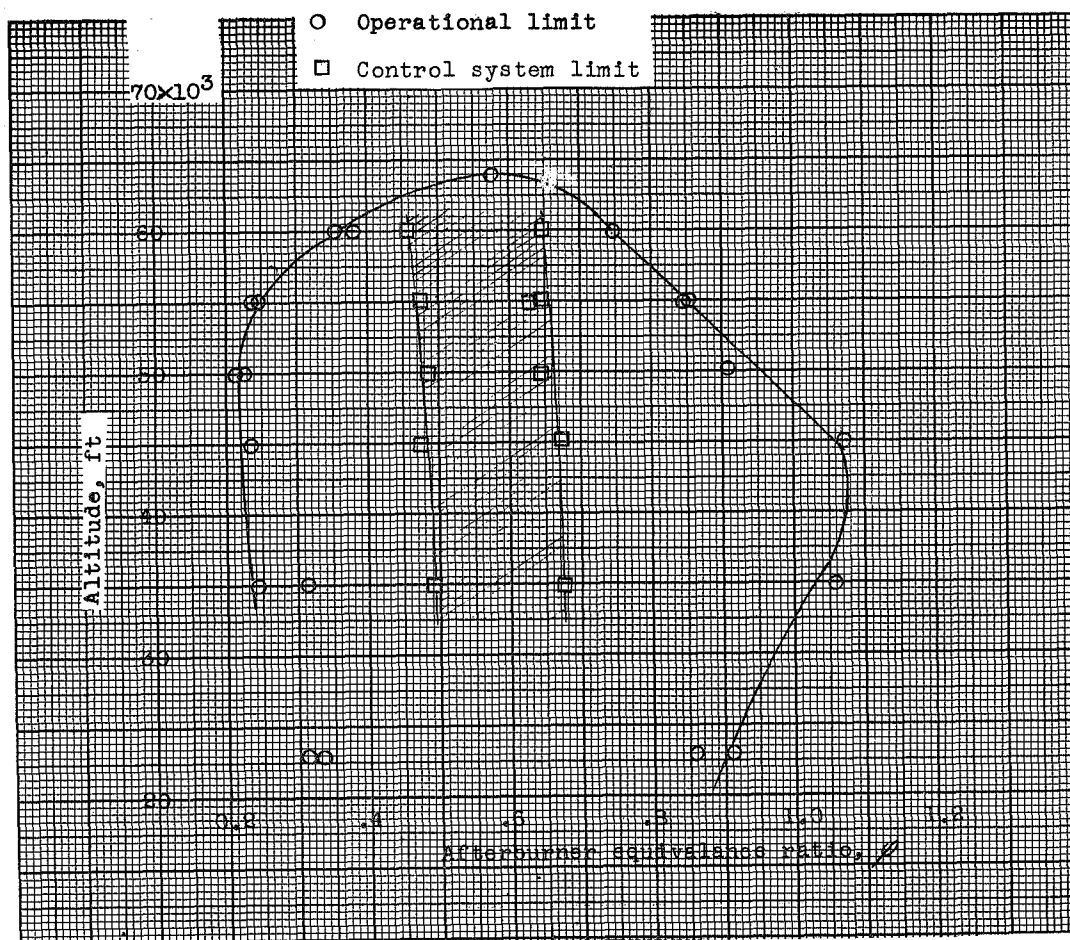


Figure 8. J71-A2 turbojet engine afterburner operational limits and afterburner control system limits of operation.

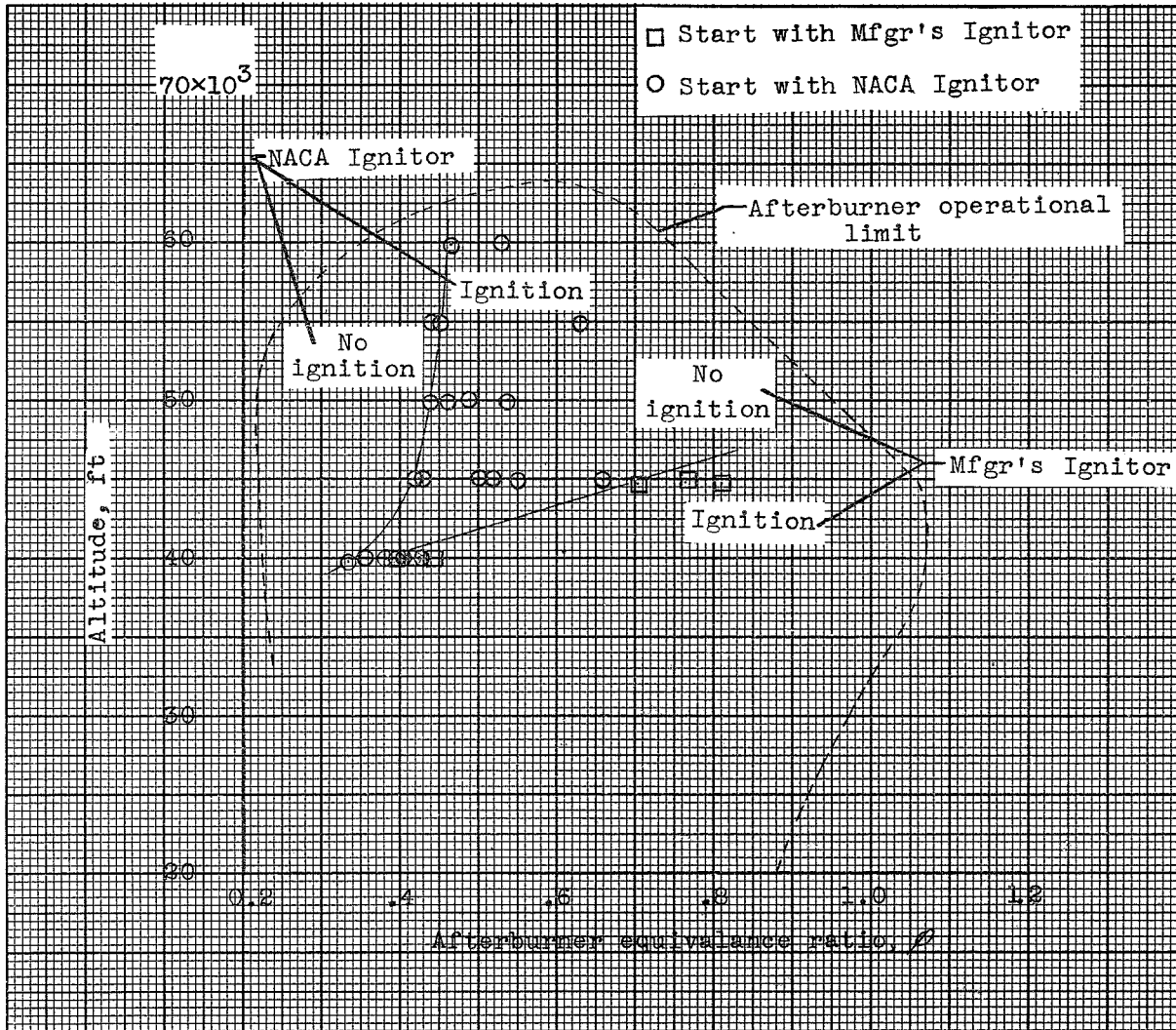


Figure 9. Area of afterburner ignition using the manufacturer's ignitor and the NACA "hot streak" ignitor.

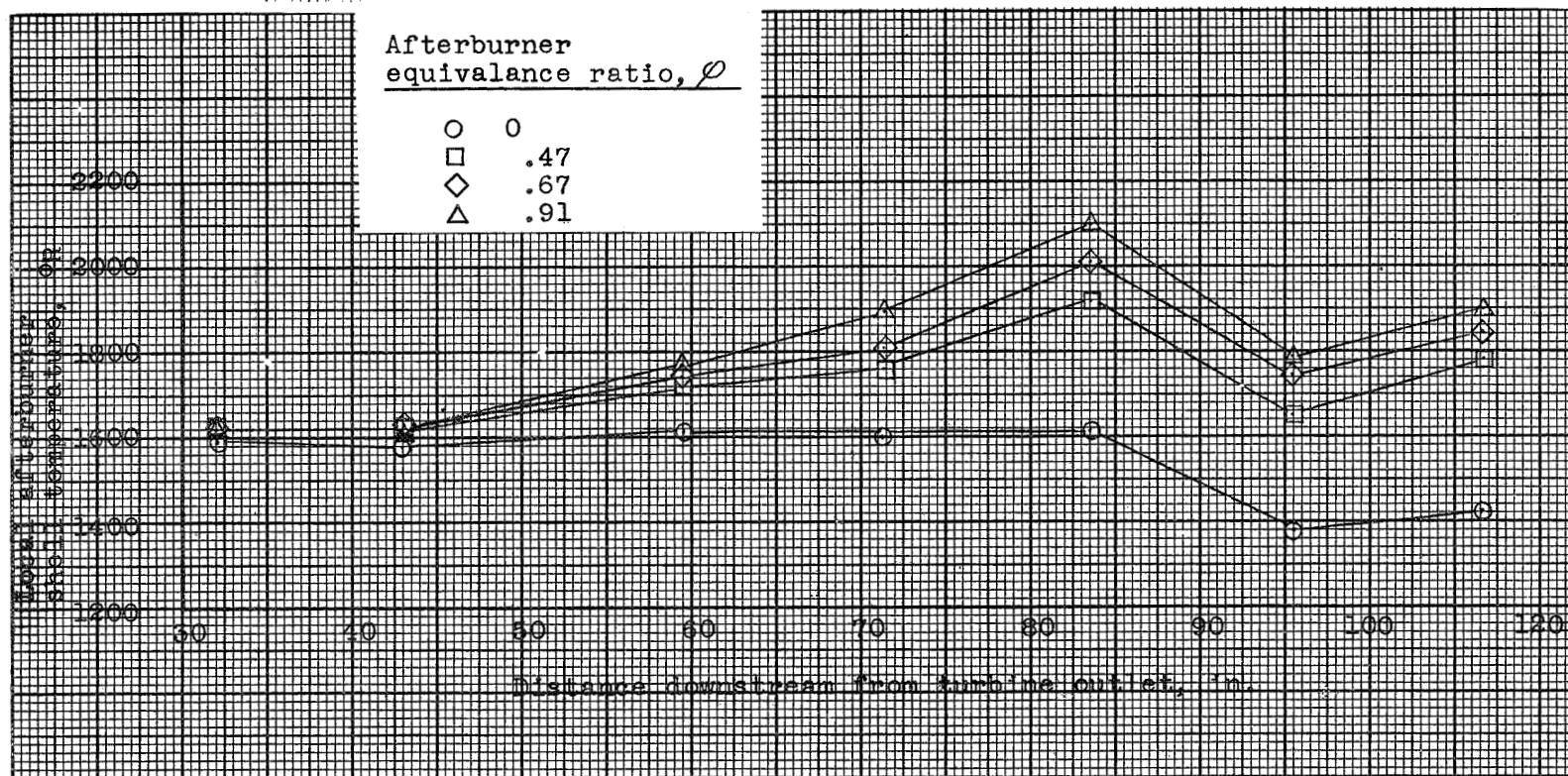
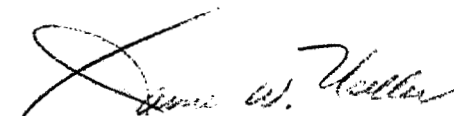


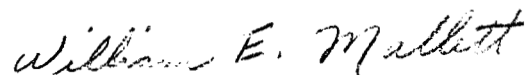
Figure 10. Local afterburner shell temperature distribution along length of the afterburner during operation at several equivalence ratios.

PRELIMINARY ALTITUDE PERFORMANCE DATA OF J71-A2

TURBOJET ENGINE AFTERBURNER

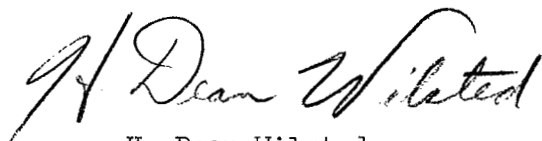


James W. Useller  
Aeronautical Research Scientist  
Propulsion Systems

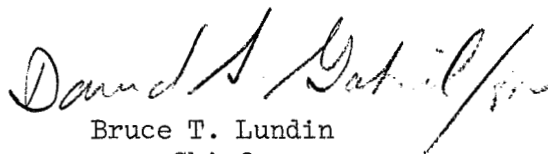


William E. Mallett  
Aeronautical Research Scientist  
Propulsion Systems

Approved:



H. Dean Wilsted  
Aeronautical Research Scientist  
Propulsion Systems



Bruce T. Lundin  
Chief  
Engine Research Division



NACA RM SE54J06

~~CONFIDENTIAL~~

FORWARD

To permit expeditious transmittal of performance data to those concerned, figures and a tabulation of "Preliminary Data" are presented herein. Preliminary Data are test data that have not received the complete analysis and extensive cross-checking normally given a set of NACA data before release.